Some Properties of Multi-Component Axion Dark Matter

Hai-Jun Li^{a,b}

^aInstitute of Theoretical Physics, Chinese Academy of Sciences, Beijing 100190, China ^bInternational Centre for Theoretical Physics Asia-Pacific, Beijing 100190, China

E-mail: lihaijun@itp.ac.cn

We introduce a mechanism for multi-component dark matter (DM) that originates from axion mixing. In this context, multi-component DM implies that the cold DM is composed of the QCD axion and many ultra-light axion-like particles (ALPs). This framework can be realized in the type IIB string axiverse with hierarchical axion masses and decay constants. Our investigation reveals that in the light QCD axion scenario, the energy density of the lightest ALP often dominates after mixing, invalidating the canonical light axion scenario. On the other hand, in the heavy QCD axion scenario, both the QCD axion and non-lightest ALPs may dominate, depending on the ALP decay constants. Under certain conditions, the canonical heavy axion scenario remains valid. Finally, we briefly discuss a theoretical framework featuring $\sim \mathcal{O}(100)$ axions, with hierarchical axion masses and decay constants.

1 Introduction

Evidence for dark matter (DM) has been accumulating for a long time, yet its true nature remains unknown. The lack of supersymmetric signals at the LHC has undermined weakly interacting massive particle (WIMP) as a prime candidate, broadening the range of possibilities, with the axion somewhat taking its place. See ref. [1] for a recent review on DM.

The axion, often referred to as the QCD axion, was originally postulated through the Peccei-Quinn (PQ) mechanism, which was devised to dynamically resolve the strong CP problem in the Standard Model (SM) [2–5]. Furthermore, a substantial quantity of ultra-light axion-like particles (ALPs) can emerge from higher-dimensional gauge fields, with the QCD axion candidate naturally being among them [6–9]. As is widely known, string theory predicts the existence of a plenitude of axions [10, 11], collectively referred to as the string axiverse [12–14].

In recent years, the QCD axion and ALPs have garnered widespread attention as natural candidates for cold DM due to their non-thermal production in the early Universe via the misalignment mechanism [15–17]. In the early Universe, the oscillation of a coherent axion state within its potential well can significantly contribute to the overall DM density. The equation of motion (EOM) governing this state resembles that of a damped harmonic oscillator. Here, the damping term is directly proportional to the Hubble parameter, while the restoring force is proportional to the axion mass. As the Universe cools down, once the Hubble parameter becomes comparable to the axion mass, the system transitions from an overdamped regime, where oscillations are heavily suppressed, to an underdamped regime, characterized by the onset of sustained oscillations. These oscillations are pivotal, as they provide a plausible explanation for the observed abundance of cold DM. See e.g. refs. [18, 19] for reviews.

For QCD axion DM, assuming an initial misalignment angle of order unity, the aforementioned misalignment mechanism imposes an upper limit on the classical QCD axion window, given by $f_a \lesssim 10^{11} - 10^{12} \,\text{GeV}$, where f_a represents the QCD axion decay constant. In other words, one of the challenges for QCD axion DM is the issue of overproduction; this problem arises when considering an axion decay constant larger than $10^{12} \,\text{GeV}$ [19]. In addition, if we consider the recently proposed dark dimension scenario [20], in which the QCD axion decay constant is constrained to a narrow range $f_a \sim 10^9 - 10^{10} \,\text{GeV}$, then QCD axion DM will face the problem of insufficient abundance [21, 22]. However, both of these issues concerning the QCD axion DM can be naturally explained through axion mixing. In the light QCD axion scenario [23, 24], the abundance of the QCD axion can be effectively suppressed, whereas in the heavy QCD axion scenario [25], its abundance can be significantly enhanced. It should be

noted that, in this context, axion mixing generally refers to the mixing between two axions, namely the mass mixing effect between the QCD axion and an ALP [26–29]. See also ref. [30] for a recent discussion on multi-axion mixing, which involves one QCD axion and multiple ultra-light ALPs.

In this work, we introduce a mechanism for multi-component DM, which arises from multi-axion mixing, and examine some of its defining properties. To begin with, we review the single-component DM scenario, involving the QCD axion and ALP, via the misalignment mechanism. Subsequently, we shift our attention to the multicomponent axion DM scenario. Here multi-component DM implies that the cold DM is constituted by a combination of the QCD axion and many ultra-light ALPs. In the simplest two-component axion DM framework, the light QCD axion scenario is no longer valid because the energy density of the mixed ALP becomes dominant, while the heavy QCD axion scenario remains valid. Expanding our analysis to multi-component axion DM frameworks, we find that in the light QCD axion scenario, the energy density of the lightest ALP often dominates after mixing, invalidating the canonical light axion scenario. In contrast, in the heavy QCD axion scenario, both the QCD axion and non-lightest ALPs can potentially dominate the energy density, depending on the relationships between the decay constants of the ALPs. Under specific conditions, the canonical heavy axion scenario maintains its validity. Finally, we briefly discuss a theoretical framework that incorporates $\sim \mathcal{O}(100)$ axions, with hierarchical axion masses and decay constants in the type IIB string axiverse.

The rest of this paper is structured as follows. In section 2, we briefly review the single-component axion DM scenario via the misalignment mechanism. In section 3, we delve into the multi-component axion DM scenario. In section 4, we briefly discuss a multi-axion framework with hierarchical axion masses and decay constants. Finally, the conclusion is given in section 5.

2 Single-component axion dark matter

In this section, we briefly review the single-component axion DM scenario, encompassing both the QCD axion and ALP DM, via the misalignment mechanism. It is important to note that in this work, we solely focus on the pre-inflationary scenario in which the PQ symmetry is spontaneously broken during inflation.

According to the misalignment mechanism [15–17], in the single-component axion DM scenario, the present energy density of the QCD axion (a_0) and the ALP¹ (A_1) can

¹Notice that the ALP discussed here is a single-field particle with a constant mass. For the sake of convenience in subsequent discussions, we denote it as A_i , and we can set i = 1 in this section.

be respectively expressed as [28]

QCD axion:
$$\rho_{a_0,0} = \frac{1}{2} m_{a_0,0} m_{a_0,\text{osc}} f_{a_0}^2 \theta_{i,a_0}^2 \left(\frac{\mathfrak{a}_{\text{osc},a_0}}{\mathfrak{a}_0} \right)^3$$
, (2.1)

ALP:
$$\rho_{A_1,0} = \frac{1}{2} m_{A_1}^2 f_{A_1}^2 \Theta_{i,A_1}^2 \left(\frac{\mathfrak{a}_{osc,A_1}}{\mathfrak{a}_0}\right)^3$$
, (2.2)

where $m_{a_0,0}$ and m_{A_1} are the QCD axion zero-temperature mass and ALP mass, respectively, f_{a_0} and f_{A_1} are the axion decay constants, θ_i and Θ_i are the initial misalignment angles, $m_{a_0,\text{osc}}$ represents the QCD axion mass at the oscillation temperature T_{osc,a_0} , $\mathfrak{a}_{\text{osc}}$ and \mathfrak{a}_0 are the scale factors at T_{osc} and at the current CMB temperature T_0 . Note that here we have not taken into account some numerical factors. For the QCD axion, in order to explain the observed DM abundance with $f_{a_0} = 1 \times 10^{12} \,\text{GeV}$, the initial misalignment angle should be $\sim \mathcal{O}(1)$. In the subsequent discussions, we will assume that the initial misalignment angles (θ_i and Θ_i) are of order one for all cases.

We find that in the single-component axion DM scenario, the ratio of the energy densities between the QCD axion and ALP is given by

$$\frac{\rho_{a_0,0}}{\rho_{A_1,0}} \simeq \frac{m_{a_0,0}}{\sqrt{m_{a_0,\text{osc}}m_{A_1}}} \left(\frac{f_{a_0}}{f_{A_1}}\right)^2. \tag{2.3}$$

Since we will later consider a model with hierarchical axion decay constants, we are more concerned about the two scenarios: either the QCD axion decay constant is significantly larger than that of the ALP, i.e., $f_{a_0} \gg f_{A_1}$, or it is significantly smaller, i.e., $f_{a_0} \ll f_{A_1}$. In both scenarios, we find that different axions dominate in the single-component axion DM scenario:

$$f_{a_0} \gg f_{A_1}$$
: QCD axion dominated, (2.4)

$$f_{a_0} \ll f_{A_1}$$
: ALP dominated. (2.5)

Notice that in this context, "dominated" merely indicates which scenario has a greater axion energy density between the two. It should not be confused with the subsequent multi-component axion DM scenarios, where "dominated" truly signifies which axion energy density is dominant.

We close this section with a brief discussion of axion mixing in the single-component axion DM scenario. Axion mixing has been extensively discussed within multi-axion frameworks, particularly in the scenario involving two axions — one QCD axion and one ALP. In these frameworks, the axion decay constants are considered to be hierarchical, with $f_{a_0} \gg f_{A_1}$ corresponding to the light QCD axion scenario [23, 24], and $f_{a_0} \ll f_{A_1}$ corresponding to the heavy QCD axion scenario [25]. It is important to note that while

the mixing of two axions is considered in that context, ultimately, only the abundance of a single axion, namely the QCD axion, is taken into account, whereas the abundance of the ALP is not considered. Therefore, we believe it is necessary to account for the energy densities of both, which is also the focus of this work. Additionally, we have recently investigated the mixing of multiple axions, where the number of axions exceeds two, typically consisting of one QCD axion and multiple ALPs [30]. Hence, another key emphasis of this work is to study the axion energy densities in such multi-axion mixing scenarios.

3 Multi-component axion dark matter

In this section, we delve into the multi-component axion DM scenario. Here, "multi-component" implies that the DM is composed of the QCD axion and ALPs. Generally, we can consider the scenario where one QCD axion coexists with one or more ALPs — this is achievable in the string axiverse, especially in the multi-axion mixing case considered in ref. [30]. However, only the situation of QCD axion DM was briefly discussed. Therefore, this work is based on that paper but focuses on the multi-component DM scenario. In addition, the properties of QCD axion or ALP DM in the case of two-axion mixing have been discussed in previous literature, but all these discussions were based on a single-component axion DM scenario. Consequently, the nature of the multi-component axion DM we discuss here has not been explored in previous literature.

Taking into account the considerations in ref. [30], the low-energy effective potential for the multi-component axion DM model here can be expressed as

$$V_{\text{eff}} = \sum_{i} \Lambda_i^4 \left[1 - \cos\left(\sum_{j} n_{ij} \theta_j\right) \right], \qquad (3.1)$$

where θ_i , f_{θ_i} , Λ_i , and n_{ij} represent the axion angles, axion decay constants, overall scales, and domain wall numbers, respectively. Here, we consider the mixing scenario involving one QCD axion and N ALPs. Therefore, the matrix of domain wall numbers n_{ij} should be taken as a $(N+1) \times (N+1)$ matrix \mathbf{n}_{ij} , beginning with indices $\mathbf{i} = 0$ and $\mathbf{j} = 0$. More details on the mixing mechanism can be found in the original paper. Here we will focus solely on the discussion of axion energy density. In this multi-component axion DM model, the present total axion energy density can be expressed as

$$\rho_{\text{tot},0} = \rho_{a_0,0} + \sum_{i}^{N} \rho_{A_i,0} \,. \tag{3.2}$$

Notice that here, $\rho_{a_0,0}$ and $\rho_{A_i,0}$ represent the present axion energy densities after taking into account the axion mixing effect.

Next, we will separately explore scenarios for two-, three-, and multi-component axion DM, taking into account both the light and heavy QCD axion frameworks.

3.1 Two-component

We first consider the simplest two-component axion DM scenario — involving one QCD axion (a_0) and one ALP (A_1) . In this case, the present energy density of the QCD axion and ALP after mixing can be respectively expressed as [28]

QCD axion:
$$\rho_{a_0,0} = \frac{1}{2} m_{a_0,0} m_{A_1} f_{A_1}^2 \Theta_{i,A_1}^2 \left(\frac{\mathfrak{a}_{osc,A_1}}{\mathfrak{a}_0} \right)^3$$
, (3.3)

ALP:
$$\rho_{A_1,0} = \frac{1}{2} m_{A_1} m_{a_0,\text{osc}} f_{a_0}^2 \theta_{i,a_0}^2 \left(\frac{\mathfrak{a}_{\text{osc},a_0}}{\mathfrak{a}_0} \right)^3$$
. (3.4)

It is worth noting that the scenario in ref. [28] differs slightly from what we have here. In this scenario, we are considering the simplest situation of two-axion mixing. Then the ratio of the energy densities between the QCD axion and ALP is given by

$$\frac{\rho_{a_0,0}}{\rho_{A_1,0}} \simeq \frac{m_{a_0,0}\sqrt{m_{a_0,\text{osc}}}}{m_{A_1}^{3/2}} \left(\frac{f_{A_1}}{f_{a_0}}\right)^2 , \qquad (3.5)$$

where the initial misalignment angles are assumed to be of order one. We find that different axions dominate in the two-component axion DM scenario:

$$f_{a_0} \gg f_{A_1}$$
: ALP dominated, (3.6)

$$f_{a_0} \ll f_{A_1}$$
: QCD axion dominated, (3.7)

corresponding to the light and heavy QCD axion scenarios, respectively. Notice that, for the effective mixing to occur, we need to assume that the mass of the ALP is slightly smaller than the zero-temperature mass of the QCD axion [30].

Here, we need to stress once again that although the two-axion mixing effect within the single-component axion DM scenario has been previously discussed, the situation changes when considering the multi-component axion scenario. From the aforementioned equations, we find that when examining a two-component axion DM model, the light QCD axion scenario is no longer valid because the energy density of the mixed ALP becomes dominant. However, we find that the heavy QCD axion scenario remains valid in this context, as the mixed QCD axion holds a dominant position.

3.2 Three-component

In this subsection, we discuss the three-component axion DM scenario — involving one QCD axion (a_0) and two ALPs $(A_1 \text{ and } A_2, \text{ where we assume } m_{A_1} < m_{A_2} < m_{a_0,0})$. More details on axion mixing in this scenario can be found in ref. [30].

It is necessary here to present the energy densities of axions separately after mixing. We first discuss the QCD axion and need to start with the ALP A_2 . The initial energy density of A_2 at the oscillation temperature T_{osc,A_2} is expressed as

$$\rho_{A_2,\text{osc}} = \frac{1}{2} m_{A_2}^2 f_{A_2}^2 \Theta_{i,A_2}^2 \,, \tag{3.8}$$

with Θ_{i,A_2} representing the initial misalignment angle of A_2 . Subsequently, in the temperature range $T_{\times_2} < T < T_{\text{osc},A_2}$, the energy density of A_2 remains adiabatically invariant. At the temperature T_{\times_2} , where the level crossing occurs, this energy density can be characterized by

$$\rho_{A_2,\times_2} = \frac{1}{2} m_{A_2}^2 f_{A_2}^2 \Theta_{i,A_2}^2 \left(\frac{\mathfrak{a}_{osc,A_2}}{\mathfrak{a}_{\times_2}} \right)^3 , \qquad (3.9)$$

where $\mathfrak{a}_{\text{osc},A_2}$ and \mathfrak{a}_{\times_2} denote the scale factors at T_{osc,A_2} and T_{\times_2} , respectively. Following this, the energy density ρ_{A_2,\times_2} is transferred to the QCD axion. The axion energy density then stays adiabatically invariant up to the current CMB temperature T_0 . As a result, we arrive at the present QCD axion energy density

QCD axion:
$$\rho_{a_0,0} = \frac{1}{2} m_{a_0,0} m_{A_2} f_{A_2}^2 \Theta_{i,A_2}^2 \left(\frac{\mathfrak{a}_{osc,A_2}}{\mathfrak{a}_0} \right)^3$$
, (3.10)

where \mathfrak{a}_0 is the scale factor at T_0 .

Then we discuss the ALP A_2 and need to start with the ALP A_1 . The initial energy density of A_1 at the oscillation temperature T_{osc,A_1} is expressed as

$$\rho_{A_1,\text{osc}} = \frac{1}{2} m_{A_1}^2 f_{A_1}^2 \Theta_{i,A_1}^2 \,, \tag{3.11}$$

with Θ_{i,A_1} representing the initial misalignment angle of A_1 . In the temperature range $T_{\times_1} < T < T_{\text{osc},A_1}$, the energy density of A_1 is adiabatically invariant, which at the level crossing temperature T_{\times_1} is given by

$$\rho_{A_1,\times_1} = \frac{1}{2} m_{A_1}^2 f_{A_1}^2 \Theta_{i,A_1}^2 \left(\frac{\mathfrak{a}_{osc,A_1}}{\mathfrak{a}_{\times_1}} \right)^3. \tag{3.12}$$

Subsequently, the energy density ρ_{A_1,\times_1} is transferred to the QCD axion and stays adiabatically invariant up to the temperature T_{\times_2} . We can obtain the corresponding QCD axion energy density

$$\rho_{a_0,\times_2} = \frac{1}{2} m_{A_1} m_{A_2} f_{A_1}^2 \Theta_{i,A_1}^2 \left(\frac{\mathfrak{a}_{osc,A_1}}{\mathfrak{a}_{\times_2}} \right)^3.$$
 (3.13)

After T_{\times_2} , the energy density ρ_{A_0,\times_2} is transferred to the ALP A_2 and stays adiabatically invariant up to T_0 . Therefore, we arrive at the present A_2 energy density

ALP
$$A_2$$
: $\rho_{A_2,0} = \frac{1}{2} m_{A_1} m_{A_2} f_{A_1}^2 \Theta_{i,A_1}^2 \left(\frac{\mathfrak{a}_{osc,A_1}}{\mathfrak{a}_0} \right)^3$. (3.14)

Next we discuss the ALP A_1 and need to start with the QCD axion a_0 . The initial energy density of a_0 at the oscillation temperature T_{osc,a_0} is expressed as

$$\rho_{a_0,\text{osc}} = \frac{1}{2} m_{a_0,\text{osc}}^2 f_{a_0}^2 \theta_{i,a_0}^2.$$
(3.15)

In the temperature range $T_{\times_1} < T < T_{\text{osc},a_0}$, the energy density of a_0 is adiabatically invariant, which at the level crossing temperature T_{\times_1} is given by

$$\rho_{a_0,\times_1} = \frac{1}{2} m_{A_1} m_{a_0,\text{osc}} f_{a_0}^2 \theta_{i,a_0}^2 \left(\frac{\mathfrak{a}_{\text{osc},a_0}}{\mathfrak{a}_{\times_1}} \right)^3 . \tag{3.16}$$

Then the energy density ρ_{a_0,\times_1} is transferred to the ALP A_1 and stays adiabatically invariant up to the temperature T_0 . Therefore, we arrive at the present A_1 energy density

ALP
$$A_1$$
: $\rho_{A_1,0} = \frac{1}{2} m_{A_1} m_{a_0,\text{osc}} f_{a_0}^2 \theta_{i,a_0}^2 \left(\frac{\mathfrak{a}_{\text{osc},a_0}}{\mathfrak{a}_0} \right)^3$, (3.17)

which is analogous to the situation considered in the two-component axion DM scenario, as shown in eq. (3.4).

Now the ratios of the energy densities between the QCD axion and ALPs are respectively expressed as

$$\frac{\rho_{a_0,0}}{\rho_{A_2,0}} \simeq \frac{m_{a_0,0}\sqrt{m_{A_1}}}{m_{A_2}^{3/2}} \left(\frac{f_{A_2}}{f_{A_1}}\right)^2, \tag{3.18}$$

$$\frac{\rho_{a_0,0}}{\rho_{A_1,0}} \simeq \frac{m_{a_0,0}\sqrt{m_{a_0,\text{osc}}}}{m_{A_1}\sqrt{m_{A_2}}} \left(\frac{f_{A_2}}{f_{a_0}}\right)^2 , \qquad (3.19)$$

$$\frac{\rho_{A_2,0}}{\rho_{A_1,0}} \simeq \frac{m_{A_2}\sqrt{m_{a_0,\text{osc}}}}{m_{A_1}^{3/2}} \left(\frac{f_{A_1}}{f_{a_0}}\right)^2 , \qquad (3.20)$$

where the initial misalignment angles are assumed to be of order one. We find that different axions dominate in the three-component axion DM scenario:

$$f_{a_0} \gg f_{A_1} \sim f_{A_2}$$
: ALP A_1 dominated, (3.21)

$$f_{a_0} \ll f_{A_1} \sim f_{A_2}$$
: QCD axion and ALP A_2 dominated, (3.22)

corresponding to the light and heavy QCD axion scenarios, respectively. It should be noted that, according to ref. [30], all the ALP decay constants here are either simultaneously smaller than the QCD axion decay constant or simultaneously larger than it. We find that in the light QCD axion scenario, only the ALP A_1 is dominant. In contrast, in the heavy QCD axion scenario, there are two distinct cases depending on the relationship between the decay constants of the ALPs A_1 and A_2 . Specifically, when f_{A_2} is significantly larger than f_{A_1} , the QCD axion is dominant. Conversely, when f_{A_2} is significantly smaller than f_{A_1} , the ALP A_2 is dominant. This can be represented as follows:

$$f_{a_0} \ll f_{A_1} \ll f_{A_2}$$
: QCD axion dominated, (3.23)

$$f_{a_0} \ll f_{A_2} \ll f_{A_1}$$
: ALP A_2 dominated. (3.24)

Notice that in the light QCD axion scenario, regardless of whether f_{A_2} is larger or smaller than f_{A_1} , the ALP A_1 remains dominant.

When comparing the two-component and three-component axion DM scenarios, in the light QCD axion framework, there is always only one ALP that dominates. Consequently, the canonical light axion scenario is no longer valid here. For the canonical heavy QCD axion scenario to remain valid within the three-component axion DM model, it is required that f_{A_1} is significantly smaller than f_{A_2} .

3.3 Multi-component

In this subsection, we discuss the more general multi-component axion DM scenario—involving one QCD axion (a_0) and many ALPs (A_i) , where we assume $m_{A_i} < m_{A_{i+1}} < m_{a_0,0}$, $\forall i$). See also ref. [30] for more details on axion mixing.

In this case, as previously derived, the present energy density of the QCD axion and ALPs after mixing can be respectively expressed as

QCD axion:
$$\rho_{a_0,0} = \frac{1}{2} m_{a_0,0} m_{A_N} f_{A_N}^2 \Theta_{i,A_N}^2 \left(\frac{\mathfrak{a}_{osc,A_N}}{\mathfrak{a}_0} \right)^3$$
, (3.25)

ALP
$$A_N$$
: $\rho_{A_N,0} = \frac{1}{2} m_{A_{N-1}} m_{A_N} f_{A_{N-1}}^2 \Theta_{i,A_{N-1}}^2 \left(\frac{\mathfrak{a}_{osc,A_{N-1}}}{\mathfrak{a}_0} \right)^3$, (3.26)

ALP
$$A_{N-1}$$
: $\rho_{A_{N-1},0} = \frac{1}{2} m_{A_{N-2}} m_{A_{N-1}} f_{A_{N-2}}^2 \Theta_{i,A_{N-2}}^2 \left(\frac{\mathfrak{a}_{osc,A_{N-2}}}{\mathfrak{a}_0} \right)^3$, (3.27)

ALP A_2 : $\rho_{A_2,0} = \frac{1}{2} m_{A_1} m_{A_2} f_{A_1}^2 \Theta_{i,A_1}^2 \left(\frac{\mathfrak{a}_{osc,A_1}}{\mathfrak{a}_0} \right)^3$, (3.28)

ALP
$$A_1$$
: $\rho_{A_1,0} = \frac{1}{2} m_{A_1} m_{a_0,\text{osc}} f_{a_0}^2 \theta_{i,a_0}^2 \left(\frac{\mathfrak{a}_{\text{osc},a_0}}{\mathfrak{a}_0} \right)^3$, (3.29)

where m_{A_N} , f_{A_N} , and Θ_{i,A_N} represent the mass, the decay constant, and the initial misalignment angle of the ALP A_N , respectively. Then the ratios of the energy densities between the QCD axion and ALPs are given by

$$\frac{\rho_{a_0,0}}{\rho_{A_N,0}} \simeq \frac{m_{a_0,0}\sqrt{m_{A_{N-1}}}}{m_{A_N}^{3/2}} \left(\frac{f_{A_N}}{f_{A_{N-1}}}\right)^2 , \qquad (3.30)$$

$$\frac{\rho_{a_0,0}}{\rho_{A_{N-1},0}} \simeq \frac{m_{a_0,0}\sqrt{m_{A_{N-2}}}}{m_{A_{N-1}}\sqrt{m_{A_N}}} \left(\frac{f_{A_N}}{f_{A_{N-2}}}\right)^2, \tag{3.31}$$

:

$$\frac{\rho_{a_0,0}}{\rho_{A_2,0}} \simeq \frac{m_{a_0,0}\sqrt{m_{A_1}}}{m_{A_2}\sqrt{m_{A_N}}} \left(\frac{f_{A_N}}{f_{A_1}}\right)^2, \tag{3.32}$$

$$\frac{\rho_{a_0,0}}{\rho_{A_1,0}} \simeq \frac{m_{a_0,0}\sqrt{m_{a_0,\text{osc}}}}{m_{A_1}\sqrt{m_{A_N}}} \left(\frac{f_{A_N}}{f_{a_0}}\right)^2 , \qquad (3.33)$$

$$\frac{\rho_{A_N,0}}{\rho_{A_{N-1},0}} \simeq \frac{m_{A_N}\sqrt{m_{N-2}}}{m_{A_N-1}^{3/2}} \left(\frac{f_{A_{N-1}}}{f_{A_{N-2}}}\right)^2, \tag{3.34}$$

:

$$\frac{\rho_{A_3,0}}{\rho_{A_2,0}} \simeq \frac{m_{A_3}\sqrt{m_{A_1}}}{m_{A_2}^{3/2}} \left(\frac{f_{A_2}}{f_{A_1}}\right)^2 , \qquad (3.35)$$

$$\frac{\rho_{A_2,0}}{\rho_{A_1,0}} \simeq \frac{m_{A_2}\sqrt{m_{a_0,\text{osc}}}}{m_{A_1}^{3/2}} \left(\frac{f_{A_1}}{f_{a_0}}\right)^2 , \qquad (3.36)$$

where the initial misalignment angles are still assumed to be of order one. We also find that different axions dominate in the multi-component axion DM scenario:

$$f_{a_0} \gg f_{A_1} \sim \cdots \sim f_{A_N}$$
: Lightest ALP A_1 dominated, (3.37)

$$f_{a_0} \ll f_{A_1} \sim \cdots \sim f_{A_N}$$
: QCD axion and ALPs (except A_1) dominated, (3.38)

corresponding to the light and heavy QCD axion scenarios, respectively. As we discussed before, in the light QCD axion scenario, only the lightest ALP A_1 is dominant. In the heavy QCD axion scenario, both the QCD axion and the remaining ALPs have the potential to be dominant, and this depends on the relationships among the ALP decay constants. If all the ALP decay constants are very close to each other, then the QCD axion and all the ALPs (except A_1) are dominant. If there are significant differences among the ALP decay constants, it will lead to different axions being dominant, and this requires an analysis based on specific model parameters.

In figures 1 and 2, we present schematic diagrams of the energy density ratio distributions in the light and heavy QCD axion scenarios, respectively. In general,

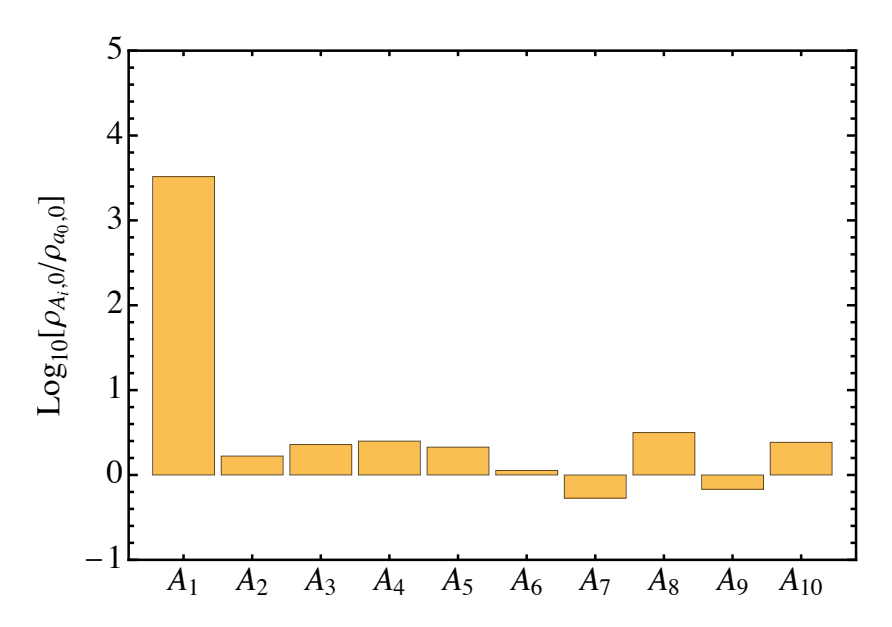


Figure 1: The ratios of the energy densities $\rho_{A_i,0}/\rho_{a_0,0}$ in the light QCD axion scenario. Here, we set $f_{a_0} = 10^{12} \,\text{GeV}$, and f_{A_i} consist of 10 random numbers within the range of $10^{9.5} - 10^{10.5} \,\text{GeV}$. Notice that we have neglected the contribution of axion masses in this context.

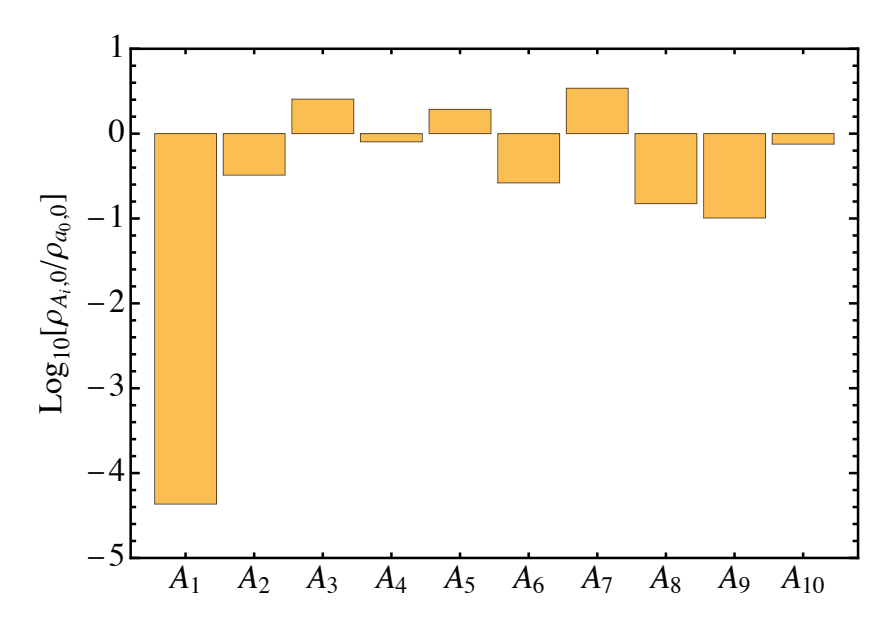


Figure 2: Same as figure 1 but for the heavy QCD axion scenario. Here, we set $f_{a_0} = 10^{12} \,\text{GeV}$, and f_{A_i} consist of 10 random numbers within the range of $10^{13.5} - 10^{14.5} \,\text{GeV}$.

within the light QCD axion scenario, the energy density of the lightest ALP tends to dominate after mixing, rendering the canonical light QCD axion scenario no longer valid. In contrast, in the heavy QCD axion scenario, both the QCD axion and ALPs (non-lightest ones) can potentially dominate, depending on the relationships between the decay constants of the ALPs. Under specific circumstances, the canonical heavy QCD axion scenario remains valid.

4 A framework with hierarchical axion masses and decay constants

In this section, we briefly discuss a multi-axion framework with hierarchical axion masses and decay constants in the type IIB string axiverse.

The explicit multi-axion models within the type IIB string axiverse are discussed in detail in ref. [14], covering scenarios involving one QCD axion and one to two light ALPs. Furthermore, in a recent ref. [31], we observe that multi-axion models with approximately $\mathcal{O}(100)$ axions are also achievable. In this case, the axion masses and decay constants exhibit a logarithmic distribution rather than a power-law one. Specifically, the geometric requirement is the existence of two blow-up modes: one $(D_{\rm SM})$ to accommodate the SM and another $(D_{\rm np})$ to support non-perturbative effects. One can consider the internal volume

$$\mathcal{V} = \frac{1}{6} \sum_{i,j,k=1}^{h^{1,1}-2} k_{ijk} t_i t_j t_k - \gamma_{\text{SM}} \tau_{\text{SM}}^{3/2} - \gamma_{\text{np}} \tau_{\text{np}}^{3/2},$$
(4.1)

where $h^{1,1}$ is the number of Kähler moduli, k_{ijk} are the intersection numbers, t_i are 2-cycle volumes, τ_i are 4-cycle moduli, and γ_i are coefficients. The leading contributions to the scalar potential arise from the corrections to Kähler potential K and superpotential W, which stabilize three moduli V, τ_{np} , and θ_{np} .

Since the axion θ_{np} is too heavy, we need to consider stabilizing the remaining Kähler moduli by incorporating additional subleading contributions to K and W. The total potential can be expressed as [31]

$$V_{\text{tot}} = V_{\text{LVS}}(\mathcal{V}) + V_F(\mathcal{V}, t_i), \qquad (4.2)$$

where V_{LVS} represents the LARGE volume scenario (LVS) potential, and V_F represents the F-term contribution. The resulting axiverse features a perfect QCD axion θ_{SM} along with multiple ultra-light ALPs, and their masses are respectively given by

QCD axion:
$$m_{a_0,0} \simeq \frac{\Lambda_{\text{QCD}}^2}{f_{a_0}}$$
, (4.3)

ALPs:
$$m_{A_i} \simeq M_p e^{-\pi \tau_i/\mathfrak{n}_i}$$
, (4.4)

where Λ_{QCD} represents the scale of QCD confinement effects that yield the axion potential, M_p is the Planck mass, and \mathfrak{n}_i determines the periodicity of the cosine potential featuring a discrete shift symmetry. The corresponding axion decay constants are respectively given by

QCD axion:
$$f_{a_0} = \frac{c_{\text{SM}}}{\tau_{\text{SM}}^{1/4}} \frac{M_p}{\mathcal{V}^{1/2}},$$
 (4.5)

ALPs:
$$f_{A_i} = \frac{c_i}{h_i} \frac{M_p}{\mathcal{V}^{2/3}}$$
, (4.6)

where $c_{\rm SM}$ and c_i are coefficients of order unity, and h_i are functions of the intersection numbers and the topological quantities. When considering a scenario where the number of axions is of order $\sim \mathcal{O}(100)$, we should focus only on the region where $\mathcal{V} \gtrsim \mathcal{O}(10^{14})$, thereby obtaining a perfect QCD axion decay constant at the TeV-scale.

Notice that in this framework, the ALPs are ultra-light, whose masses are all smaller than that of the QCD axion, which is what we anticipate in our multi-component axion DM scenario. Regarding the axion decay constants, we expect that some ALPs have decay constants smaller than that of the QCD axion, while others have decay constants larger than that of the QCD axion. This corresponds respectively to the light QCD axion and heavy QCD axion scenarios discussed in the preceding sections.

5 Conclusion

In summary, we have introduced a mechanism for multi-component DM, which arises from multi-axion mixing, and examined some of its defining properties. In this context, the multi-component axion DM scenario presents a fascinating departure from the single-component paradigm, as it posits that cold DM is composed of a combination of the QCD axion and numerous ultra-light ALPs. Through our analysis of the simplest two-component to multi-component frameworks, we uncovered significant implications in the light and heavy QCD axion scenarios. In the light QCD axion scenario, the mixing of axions often leads to the dominance of the energy density of the lightest ALP, thereby invalidating the canonical light axion scenario. On the other hand, the heavy QCD axion scenario exhibits a more nuanced picture. Here, both the QCD axion and non-lightest ALPs have the potential to dominate the energy density, depending on the relationships between the decay constants of the ALPs. Under specific conditions, the canonical heavy axion scenario can maintain its validity, suggesting that there may be room where the heavy QCD axion still plays a significant role in the DM landscape. Finally, our brief discussion of a theoretical framework that incorporates approximately $\mathcal{O}(100)$ axions within the type IIB string axiverse provides a potential foundation for

our multi-component axion DM models. The hierarchical axion masses and decay constants in this framework offer a rich playground for studying the dynamics of multi-axion systems and their implications for cold DM.

Acknowledgments

This work was partly supported by the Institute of Theoretical Physics, CAS, and partly supported by the International Centre for Theoretical Physics Asia-Pacific.

References

- [1] M. Cirelli, A. Strumia and J. Zupan, Dark Matter, 2406.01705.
- [2] R. Peccei and H. R. Quinn, CP Conservation in the Presence of Instantons, Phys. Rev. Lett. 38 (1977) 1440–1443.
- [3] R. Peccei and H. R. Quinn, Constraints Imposed by CP Conservation in the Presence of Instantons, Phys. Rev. D 16 (1977) 1791–1797.
- [4] S. Weinberg, A New Light Boson?, Phys. Rev. Lett. 40 (1978) 223–226.
- [5] F. Wilczek, Problem of Strong P and T Invariance in the Presence of Instantons, Phys. Rev. Lett. 40 (1978) 279–282.
- [6] E. Witten, Some Properties of O(32) Superstrings, Phys. Lett. B 149 (1984) 351–356.
- [7] M. B. Green and J. H. Schwarz, Anomaly Cancellation in Supersymmetric D=10 Gauge Theory and Superstring Theory, Phys. Lett. B 149 (1984) 117–122.
- [8] K.-w. Choi, A QCD axion from higher dimensional gauge field, Phys. Rev. Lett. 92 (2004) 101602, [hep-ph/0308024].
- [9] M. Reece, Extra-dimensional axion expectations, JHEP 07 (2025) 130, [2406.08543].
- [10] P. Svrcek and E. Witten, Axions In String Theory, JHEP 06 (2006) 051, [hep-th/0605206].
- [11] J. P. Conlon, The QCD axion and moduli stabilisation, JHEP 05 (2006) 078, [hep-th/0602233].
- [12] A. Arvanitaki, S. Dimopoulos, S. Dubovsky, N. Kaloper and J. March-Russell, String Axiverse, Phys. Rev. D 81 (2010) 123530, [0905.4720].
- [13] B. S. Acharya, K. Bobkov and P. Kumar, An M Theory Solution to the Strong CP Problem and Constraints on the Axiverse, JHEP 11 (2010) 105, [1004.5138].
- [14] M. Cicoli, M. Goodsell and A. Ringwald, The type IIB string axiverse and its low-energy phenomenology, JHEP 10 (2012) 146, [1206.0819].

- [15] J. Preskill, M. B. Wise and F. Wilczek, Cosmology of the Invisible Axion, Phys. Lett. B 120 (1983) 127–132.
- [16] L. Abbott and P. Sikivie, A Cosmological Bound on the Invisible Axion, Phys. Lett. B 120 (1983) 133–136.
- [17] M. Dine and W. Fischler, *The Not So Harmless Axion*, *Phys. Lett. B* **120** (1983) 137–141.
- [18] D. J. E. Marsh, Axion Cosmology, Phys. Rept. **643** (2016) 1–79, [1510.07633].
- [19] C. A. J. O'Hare, Cosmology of axion dark matter, PoS COSMICWISPers (2024) 040, [2403.17697].
- [20] M. Montero, C. Vafa and I. Valenzuela, The dark dimension and the Swampland, JHEP 02 (2023) 022, [2205.12293].
- [21] N. Gendler and C. Vafa, Axions in the dark dimension, JHEP 12 (2024) 127, [2404.15414].
- [22] H.-J. Li, QCD axion dark matter in the dark dimension, JHEP **05** (2025) 139, [2412.19426].
- [23] R. Daido, N. Kitajima and F. Takahashi, Level crossing between the QCD axion and an axionlike particle, Phys. Rev. D 93 (2016) 075027, [1510.06675].
- [24] H.-J. Li, Y.-Q. Peng, W. Chao and Y.-F. Zhou, Light QCD axion dark matter from double level crossings, Phys. Lett. B 849 (2024) 138444, [2310.02126].
- [25] D. Cyncynates and J. O. Thompson, Heavy QCD axion dark matter from avoided level crossing, Phys. Rev. D 108 (2023) L091703, [2306.04678].
- [26] C. T. Hill and G. G. Ross, Models and New Phenomenological Implications of a Class of Pseudogoldstone Bosons, Nucl. Phys. B 311 (1988) 253–297.
- [27] S.-Y. Ho, K. Saikawa and F. Takahashi, Enhanced photon coupling of ALP dark matter adiabatically converted from the QCD axion, JCAP 10 (2018) 042, [1806.09551].
- [28] H.-J. Li, Axion dark matter with explicit Peccei-Quinn symmetry breaking in the axiverse, JCAP **09** (2024) 025, [2307.09245].
- [29] K. Murai, Y. Narita, F. Takahashi and W. Yin, QCD axion dark matter from level crossing with refined adiabatic condition, JHEP 04 (2025) 124, [2412.10232].
- [30] H.-J. Li and Y.-F. Zhou, Axion Mixing in the String Axiverse, 2504.10170.
- [31] I. Broeckel, M. Cicoli, A. Maharana, K. Singh and K. Sinha, Moduli stabilisation and the statistics of axion physics in the landscape, JHEP 08 (2021) 059, [2105.02889]. [Addendum: JHEP 01, 191 (2022)].